Nanometric polythiophene films with electrocatalytic activity for non-enzymatic detection of glucose

Marcele A. Hocevar,[1,2] Georgina Fabregat,[2,3] Elaine Armelin,[2,3] Carlos A. Ferreira[1] and Carlos Alemán[2,3,*]

[1] *Universidade Federal do Rio Grande do Sul – DEMAT - Av. Bento Gonçalves, 9500 - setor 4- prédio 43426 - Cep. 91501-970 - Porto Alegre - RS – Brazil.*

[2] *Departament d'Enginyeria Química, E.T.S. d'Enginyers Industrials de Barcelona, Universitat Politécnica de Catalunya, Diagonal 647, Barcelona E-08028, Spain.*

[3] *Center for Research in Nano-Engineering, Universitat Politécnica de Catalunya, Campus Sud, Edifici C', C/Pascual I Vila s/n, Barcelona E-08028, Spain.*

[*] carlos.aleman@upc.edu.

ABSTRACT

Electrochemical detection of glucose using simple polymeric electrodes without the assistance of enzymatic or inorganic catalysts (*i.e.* metals or metal oxides) has been issued a challenge to the scientific community. In this work we present the development of a potentiometric glucose sensor based on nanometric films of a very electroactive polythiophene derivative bearing a hydroxyl substituent per repeat unit. The sensor, which is enzyme free and does not require from additional catalytic nanoparticles, exhibits excellent tolerance against interferents, a low detection limit, and a deviation lower than 2% with respect to measures in human blood samples with commercial sensors. The excellent response of this highly electroactive polythiophene derivative, which exhibits a very simple chemical structure, has been attributed to the closeness between the hydroxyl substituents and the aromatic groups contained in the linear and rigid backbone. This particular chemical distribution favors the activation of the hydroxyl substituents, inducing their participation in the oxidation of glucose molecules.

Keywords: Glucose; Polythiophene; PEDOT; Sensor

1. Introduction

Regular monitoring of glucose levels in the human body is crucial for the diagnosis and management of diabetes, which has become a worldwide public health problem. In addition, monitoring of the glucose metabolism through the detection of changes in the concentration of this important chemical may improve the treatment of brain diseases (*e.g.* brain tumors and traumatic brain injuries) [1,2].

To date the most common glucose biosensors, which are based on amperometric detection, achieve specific recognition by immobilizing an enzyme called glucose oxidase (GOx) that catalyzes the oxidation of glucose to gluconolactone [3]. Within this context the application of conducting polymers (CPs) to bioelectronic surfaces has gained considerable attention due to a number of advantages, such as their easy preparation and direct deposition on the electrode surface [4]. Thus, CPs have been successfully used to increase the signal-to-noise ratio in the detection process and to immobilize and entrap the enzymes [5-10]. For the specific case of GOx, a large number of CPs have been either functionalized or modified at their surface to facilitate the effective chemical or physical immobilization of the enzyme, enabling their subsequent utilization as amperometric sensors [11-16]. Another important advantage of these CP-based materials is that they usually minimize the access of interfering compounds to the biosensor surface.

In order to solve the problems associated to enzyme-based sensors (*e.g.* poor reproducibility, complicated immobilization processes and high cost), the development of non-enzymatic glucose sensors (NEGSs) has attracted the interest of scientists. Most NEGSs are primarily based on the ability of Au, Cu, Ni, Pt and their oxides to catalyze glucose oxidation [17-22]. Carbon nanotubes and graphene have also been used to fabricate NEGSs [23-26]. In recent years some NEGSs have been fabricated by

stabilizing catalysts with CPs, *e.g.* poly(hydroxyl-1,4-naphthoquinone) and poly(3-octylthiophene) (P3OTh) with Au, and polypyrrole (PPy) with magnetic $ZnFe_2O_4$ [17,18,27]. Although direct electroxidation of glucose is kinetically very slow and, therefore, enzymatic or inorganic catalysts are required to speed up the process and to offer adequate selectivity, Çiftçi *et al.* [28] recently developed a new CP able to detect glucose without the assistance of any catalytic agent. This sensor, which was based on poly(3-aminophenylboronic acid-co-3-octylthiophene) (PAPBAOT) deposited on glassy carbon, exhibited a detection limit of 0.5 mM and was selective against common interferents, *i.e.* uric acid (UA), ascorbic acid (AA) and dopamine (DA) [28]. In spite of this success, the commercial application of PAPBAOT is drastically limited by its complex chemical structure (Scheme 1), which includes boronic acid and alkyl spacer functional groups as molecular recognition and penetration agent, respectively.

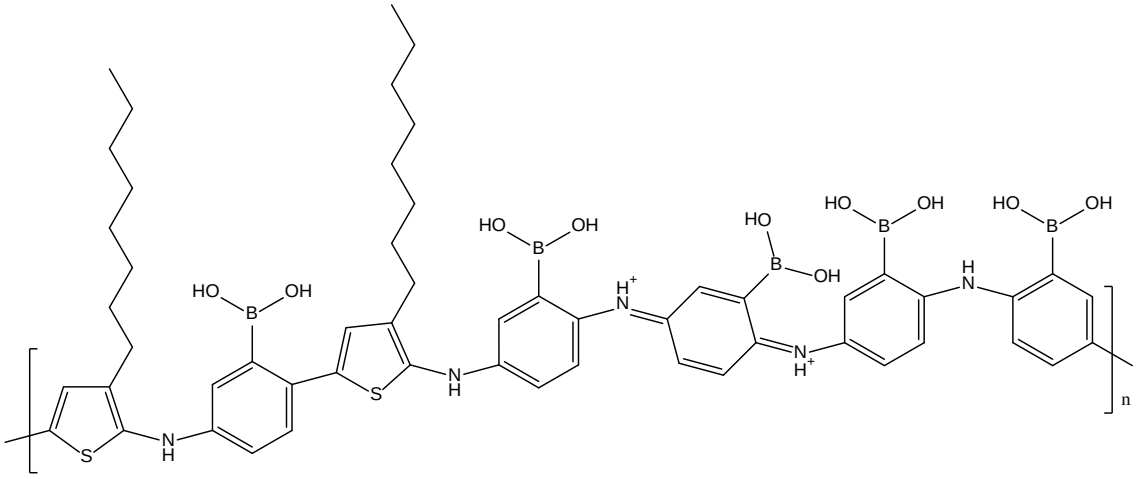

Scheme 1: Chemical structure proposed for PAPBAOT in reference 26

In this work we present a new NEGS based on a very simple CP, which was recently designed to improve the amperometric detection of DA [29]. This CP, poly(hydroxymethyl-3,4-ethylendioxythiophene) (PHMeDOT), was chosen among the vast palette of poly(3,4-ethylendioxythiophene) (PEDOT) derivatives that can be

prepared using commercial monomers because of the electrocatalytic activity of the exocyclic hydroxymethyl group (Scheme 2) [29]. The main advantages of PHMeDOT, which acts as glucose sensor without any special modification or treatment, with respect to other reported system are the lack of enzymatic or inorganic catalysts and the simplicity of its chemical structure, facilitating the synthesis process and reducing its economic cost.

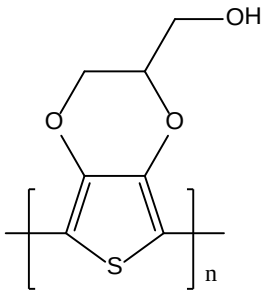

Scheme 2: Chemical structure of PHMeDOT

2. **Methods**

2.1. Materials

Thieno[3,4-b]-1,4-dioxin-2-methanol (HMeDOT) monomer, anhydrous lithium perchlorate ($LiClO_4$), D-glucose, DA hydrochloride (3-hydroxytyramine hydrochloride), AA (L-configuration, crystalline) and UA (crystalline) of analytical reagent grade were purchased from Sigma-Aldrich (Spain), while sodium citrate dehydrate was obtained from J. T. Baker. All chemicals were used without further purification. Anhydrous $LiClO_4$, analytical reagent grade, was stored in an oven at 80 ºC before use in the electrochemical trials.

Glucose oxidase (GOx) from *Aspergillus niger* (Type VII, lyophilized power) and D-glucose were purchased from Sigma Aldrich. Phosphate buffer solution (PBS) 0.1 M with pH= 7.4 was prepared as electrolyte solution by mixing four stock solutions of NaCl, KCl, $NaHPO_4$ and KH_2PO_4.

2.2. Synthesis

PHMeDOT films were produced by chronoamperometry (CA) under a constant potential of 0.80 V. A bare glassy carbon (GC) electrode with a diameter of 2 mm was used as working electrode while a silver sheet was employed as counter electrode. The reference electrode was an Ag|AgCl electrode. Films were obtained using a 0.1 M monomer aqueous solution with 0.1 M $LiClO_4$ and employing a polymerization time of 10 s. All electrochemical experiments were conducted on a PGSTAT302N AUTOLAB potenciostat-galvanostat (Ecochimie, The Netherlands) equipped with the ECD module to measure very low current densities (100 μA-100 pA), which was connected to a PC computer controlled through the GPES software.

2.3. Cyclic votammetry (CV)

CV assays were carried out using the Autolab PGSTAT302N equipment described above. Experiments were performed in a glass cell containing 100 μL of 0.1 M PBS (pH=7.4) at room temperature and equipped with saturated Ag|AgCl as reference electrode and a silver sheet as counter electrode. Voltammograms were recorded in the potential range from -0.80 to 0.50 V at a scan rate of 50 $mV \cdot s^{-1}$.

2.4. Immobilization of glucose oxidase

In addition to non-enzymatic PHMeDOT sensors, enzyme-containing glucose biosensors were prepared by immobilizing GOx on the PHMeDOT films. For this purpose, suitable amount of GOx solution (33 mg in 1 mL 0.1 M PBS solution) was prepared in a vial. After this, 1 μL of the GOx solution was dropped onto the PHMeDOT film and dried in a fridge at 6 ºC for 12 h.

2.5. Atomic force microscopy (AFM)

Topographic AFM images were obtained with a Molecular Imaging PicoSPM using a NanoScope IV controller in ambient conditions. The averaged RMS roughness (*r*) was determined using the statistical application of the Nanoscope software, which calculates the average considering all the values recorded in the topographic image with exception of the maximum and the minimum. AFM measurements were performed on various parts of the films, which produced reproducible images similar to those displayed in this work.

2.6. FTIR and UV-vis spectroscopies

FTIR spectra were recorded on a Bruker Vertex 70 FTIR spectrometer, equipped with a diamond ATR device (Golden Gate, Bruker) in transmission mode.

2.7. Scanning electron microscopy (SEM) and energy dispersive X-ray (EDX) spectroscopy

EDX spectroscopy and SEM studies were performed to examine the composition of the synthesized nanocomposites and to examine the effect of the clay on the surface morphology, respectively. Dried samples were placed in a Focussed Ion Beam Zeiss Neon 40 scanning electron microscope operating at 3 kV, equipped with an EDX spectroscopy system.

2.8. Electrochemical detection of glucose

Chronoamperometric measurements were carried out at room temperature in the reaction cell containing 100 μL of 0.1 M PBS at a polarization potential of -600 mV using the Autolab PGSTAT302N equipment described above. Glucose solutions were

prepared in 10 mM PBS and allowed to mutarotate overnight. Choroamperometric curves were obtained after adding 4 μL of a desired concentration of glucose solution under constant stirring at 100 s intervals.

AU, AA and DA were used as interfering agents for chronoamperometric detection of glucose. 25 mM solutions of these species were prepared in 10 mM PBS. Choroamperometric curves in presence of interfering agents were obtained after adding 4 μL of a 25 mM solution of each of such species under constant stirring at 100 s intervals.

3. Results and discussion

The success of the anodic polymerization process was proved by FTIR spectroscopy (Figure 1). Thus, the absence of the absorption band at 3099 cm^{-1} in the polymer spectrum is consistent with the lack of hydrogen atoms at the C^{α}-position, which are clearly detected in the monomer spectrum. This proves that the anodic polymerization of the monomers occurs at the α-α' position of the thiophene rings, providing linear molecules. The most relevant bands in the PHMeDOT spectrum are observed at 3669 cm^{1} (O–H stretching) and 2980-2900 cm^{-1} (–C–H aliphatic stretching) and 1238 cm^{-1} (-CH deformation), from CH_2 lateral groups and methylenedioxy groups. The strong and broad band vibrations at 1388 and 1059 cm^{-1} are attributed to the stretching modes of thiophene ring and ether group, respectively, while the main bands in the monomer spectrum are centered at 3208 cm^{-1} (O–H stretching), 3099 cm^{-1} (=C–H stretching), 2937-2869 cm^{-1} (–C–H stretching), 1578 cm^{-1} (C=C stretching) and 1484 to 1339 cm^{-1} (C-C thiophene ring vibrations).

PHMeDOT films polymerized with only 10 s of galvanostatic potential and electrodeposited on glass carbon (GC) electrodes had a thickness and root-mean-square

roughness, determined by scratch AFM, of 90±5 nm and 83±6 nm, respectively. SEM micrographs indicate that nanometric PHMeDOT films exhibit a granular surface morphology (Figure 2a) that closely resembles the one obtained for linear PEDOT prepared using the same experimental conditions [30]. The surface topography observed by AFM (Figure 2b) shows small clusters of aggregated molecules homogenously distributed. This corresponds to the topography typically found in heterocyclic CPs with a linear growing [31], in which molecules are exclusively formed by α-α linkages because the β-positions of the aromatic ring are locked.

The doping level, which has been roughly estimated using the Cl/S ratio derived from EDX spectroscopy (Figure 2c), is 0.87, this value being slightly higher than that of PEDOT [32]. This high oxidation degree explains the noticeably high electroactivity observed in the control voltammogram of PHMeDOT (Figure 3a). Comparison of the voltammetric response of PHMeDOT in 0.1 M phosphate buffered saline solution (PBS, pH= 7.4) as prepared and after immobilize GOx onto its surface indicates that the enzyme does not play any electro-catalytic effect in oxidation-reduction processes (Figure 3a), harming the intrinsic electrochemical behaviour of PHMeDOT.

The current response of PHMeDOT films as prepared and with GOx immobilized at the surface was compared by applying a polarization potential of -600 mV vs Ag|AgCl to a 0.1 M PBS stirred solution. For this purpose, 4μL of a 25 mM glucose solution were injected into the PBS-containing electrochemical cell, representing an effective glucose concentration of only 1 mM. The chronoamperometric response to the glucose injection of the two sensors was very similar (Figure 3b), evidencing that the PHMeDOT electrode can be directly used as a NEGS.

The presence of interfering species, such as UA, AA and DA, in biological samples can influence the performance of the sensor during the oxidation of glucose. In order to

investigate the selectivity of PHMeDOT, the chronoamperometric response of the PHMeDOT NEGS upon the successive injection of glucose and interferents into the PBS-containing cell was examined. Results (Figure 4) clearly prove that AU, AA and DA do not block the glucose signal. Moreover, superposition of the profiles obtained with and without injection of interfering species indicates that the sensitivity increases significantly in presence of interfering agents (Figure 4). Thus, the current density of the peak associated to the glucose injection at t= 600 s, after addition of interfering species, is 9 and 16 $\mu A/cm^2$ higher than the first and fourth glucose injections peaks (*i.e.* those at t= 300 and 600 s, respectively) displayed in the profile without interfering agents. These results reflect that the PHMeDOT NEGS can be successfully used in presence of interfering agents, offering analytical selectivity to the sensor.

Figure 5 plots the oxidation peak current density versus glucose concentration (eight different measures for each concentration using the standard addition method). A linear relationship between the current density and the glucose concentration was established in the concentration range from 1 to 9 mM (R^2= 0.963), and a sensitivity of 2.241 $\mu A/cm^2$ was obtained from the slope in the linear range. When the concentration is above 9 mM, deviation from linearity is detected, presumably due to a change from mass transport controlled to kinetically controlled current at concentrations higher than 9 mM. The detection limit, which was calculated on the basis of signal to noise ratio of 3, was 0.9 mM.

PHMeDOT NEGSs are comparable in terms of sensitivity and selectivity to other sensors reported in the literature. For example, the detection limit of non-enzymatic PAPBAOT (Scheme 1), which exhibits a very complex chemical structure, is 0.5 mM [28]. Other representative NEGSs are P3OTh functionalized with Au NPs [18] and PPy with Cu_xO NPs [22], which exhibit a detection limit of 0.2 and 6.2 mM, respectively.

Accordingly, when compared to other biosensors the superiority of PHMeDOT rests on its simplicity, which is based on the substitution of the electrocatalytic activity associated to the GOx and/or inorganic agents by that of the exocyclic hydroxyl groups. Thus, comparison between FTIR spectra recorded for the polymer and the monomer evidences a red shift for the O–H stretching vibration (Figure 1). This has been attributed to a reduction of the intermolecular polymer···polymer hydrogen bonds [33], which facilitates the accessibility of hydroxyl side groups and, therefore, their participation in the catalysis of the glucose oxidation. Thus, the closeness of the hydroxyl groups to the electroactive polythiophene backbone, combined with such accessibility, favors their activation in response to the application of the electric potential inducing their participation as catalyst in the global reaction mechanism. It should be noted that the backbone planarity and by extension the backbone rigidification of PEDOT derivatives are due to the restrictions imposed by the fused dioxane ring and to the electron-donating effects provided by the oxygen atoms contained in such cyclic substituent, as was recently proved by quantum mechanical calculations [34]. The π-conjugation of the planar *anti* conformation induced by the dioxane ring and the above mentioned electron-donating effects provided by the oxygen atoms attached to the positions three and four of each thiophene ring give a significant gain in aromaticity and more favorable electrostatic interactions [34]. This feature explains the excellent electronic properties of PHMeDOT backbone, which play a very important role in the activation of hydroxyl catalytic effects.

Finally, the applicability of the PHMeDOT NEGSs was examined by considering real blood samples extracted from two different individuals. Measures were performed depositing 2 drops of blood directly onto the surface of the electrode, applying a polarization potential of -600 mV, and, enabling equilibration of the current density

(Figure 6). Results, which were obtained by applying the calibration curve displayed in Figure 5, are compared in Table 1 with those obtained using the OneTouch UltraMini® blood glucose meter, commercialized by the Johnson&Johnson company (Figure 6, insets). The glucose concentrations determined using the PHMeEDOT NEGSs differ by less than 2% from those concentrations measured using the commercial sensor, proving again the excellent performance of this CP-based sensor.

4. Conclusions

In summary, the application of PHMeDOT nanometric films for the electrochemical detection of glucose in absence of enzymatic or inorganic catalytic agents has been explored. Overall results indicate that PHMeDOT behaves a NEGS with good activity towards the determination of glucose with the linear concentration range of 1-9 mM. The sensor is effective in presence of UA, AA and DA interfering agents. In spite of its simple chemical structure, PHMeDOT performance is comparable to those obtained using more sophisticated and commercial sensors. In addition to its simplicity, other important advantages of this hydroxylated NEGS are its electrochemical stability and ease of fabrication. The excellent response of PHMeDOT has been attributed to a combination of the backbone aromatic properties and the closeness between the hydroxyl groups and the thiophene ring. These features facilitate the activation of the hydroxyl groups, which promotes the oxidation of glucose molecules without the assistance of enzymatic or inorganic catalytic agents.

In summary, the advantageous features exhibited by the proposed polythiophene derivative hold the promise for the development of a cost-effective practicable application in a near future.

Acknowledgements

Authors acknowledge MINECO-FEDER (MAT2015-69367-R) for financial support. G.F. is thanked for the financial support through a postdoc-UPC. M. A. H. thanks the Brazilian government agencies CNPq and CAPES (process BEX 7986/14-9) which provided the financial support for scholarship. Support for the research of C.A. was received through the prize “ICREA Academia” for excellence in research funded by the Generalitat de Catalunya.

References

[1] C. K. N. Li, C. K. N. Cancer 50 (1982) 2066–2073.

[2] M. De Fazio, R. Rammo, K. O’Phelan, M. R. Bullock, Neurocrit. Care 14 (2011) 91–96.

[3] R. Gifford, Chem. Phys. Chem. 14 (2013) 2032–2044.

[4] A. Murat, Mater. Sci. Eng. C 33 (2013) 1853–1859.

[5] M. Martí, G. Fabregat, F. Estrany, C. Alemán, E. Armelin, J. Mater. Chem. 20 (2010) 10652–10660.

[6] M. J. Higgins, P. J. Molino, Z. L. Yue, G. G. Wallace, Chem. Mater. 24 (2012) 828–839.

[7] G. Fabregat, E. Armelin, C. Alemán, J. Phys. Chem. B 118 (2014) 4669–4682.

[8] S. Cosnier, M. Holzinger, Chem. Rev. 40 (2011) 2146–2159.

[9] D. López-Pérez, D. Aradilla, L. J. del Valle, C. Alemán, J. Phys. Chem. C 117 (2013) 6607–6619.

[10] M. Singh, P. K. Kathuroju, N. Jampana, Sensor Actuat. B Chem. 143 (2009) 430–443.

[11] T. Ceren, S. Soylemez, M. Kesik, H. Unay, S. Sayin, H. B. Yildiz, A. Cirpan, L. Toppare, RSC Adv. 5 (2015) 35940–35947.

[12] S. Cosnier, Biosens. Bioelectron. 14 (1999) 443–456.

[13] F. B. Emre, F. Ekiz, A. Balan, S. Emre, S. Timur, L. Toppare, Sens. Actuators B 158 (2011) 117–123.

[14] S. Soylemez, F. E. Kanik, M. Ileri, S. O. Hacioglu, L. Toppare, Talanta 118 (2014) 84.

[15] A. L. Goff, M. Holzinger, S. Cosnier, Analyst 136 (2011) 1279–1287.

[16] M. Kesik, F. E. Kanik, G. Hizalan, D. Kozanoglu, E. N. Esenturk, S. Timur, L. Polymer 54 (2013) 4463–4471.

[17] M. C. D. Cooray, Y. Liu, S. J. Langford, A. M. Bond, J. Zhang, Anal. Chim. Acta 856 (2015) 27–34.

[18] H. Çiftçi, U. Tarmer, React. Funct. Polym. 72 (2012) 127–132.

[19] Y. Fu, F. Liang, H. Tian, J. Hu, Electrochim. Acta 120 (2014) 314–320.

[20] R. Ahmad, M. Vaseem, N. Tripathy, Y.-B. Hahn, Anal. Chem. 85 (2013) 10448–10454.

[21] J. Wang, W. D. Zhang, Electrochim. Acta, 56 (2011) 7510–7516.

[22] F. Meng, W. Shi, Y. Sun, X. Zhu, G. Wu, C. Ruan, X. Liu, D. Ge, Biosens. Bioelectron. 42 (2013) 141–147.

[23] K. B. Male, S. Hrapovic, Y. Liu, D. Wang, J. H. T. Luong, Anal. Chim. Acta 516 (2004) 35–41.

[24] J. Yang, W.-D. Zhang, S. Gunasekaran, S. Biosens. Bioelectron. 26 (2010) 279–284.

[25] W. Lei, W. Si, Y. Xu, Z. Gu, Q. Hao, Microchim. Acta 181 (2014) 707–722.

[26] P. M. Nia, F. Lorestani, P. M. Woi, Y. Alias, Appl. Surf. Sci. 332 (2015) 648–656.

[27] Z. Shahnavaz, F. Lorestani, Y. Alias, P. M. Woi, Appl. Surf. Sci. 317 (2014) 622–629.

[28] H. Çiftçi, U. Tarmer, Electrochim. Acta 90 (2013) 358–365.

[29] G. Fabregat, J. Casanovas, E. Redondo, E. Armelin, C. Alemán, Phys. Chem. Chem. Phys. 16 (2014) 7850–7861.

[30] D. Aradilla, D. Azambuja, F. Estrany, M. T. Casas, C. A. Ferreira, J. Mater. Chem. 22 (2012) 13110–13122.

[31] D. Aradilla, F. Estrany, E. Armelin, C. Alemán, Thin Solid Films 518 (2010) 4203–4210.

[32] C. Ocampo, R. Oliver, E. Armelin, C. Alemán, F. Estrany, J. Polym. Res. 13 (2006) 193–200.

[33] J. Casanovas, O. Bertran, E. Armelin, J. Torras, F. Estrany, C. Alemán, J. Phys. Chem. A 112 (2008) 10650–10656.

[34] J. Poater, M. Solà, J. Casanovas, C. Alemán, J. Phys. Chem. A 114 (2010) 1023–1028.

Table 1. Blood glucose level measured for two different individuals using the PHMeDOT NEGSs and commercial OneTouch UltraMini® blood glucose meters.

	Individual 1 (mg/dL)	Individual 1 (mg/dL)
PHMeDOT NEGS	90.96	122.81
OneTouch UltraMini®	90	125
Deviation (in %)	+1.07	-1.75%

CAPTIONS TO FIGURES

Figure 1. FTIR spectra of (a) PHMeDOT and (b) the HMeDOT monomer.

Figure 2. (a) SEM micrograph, (b) AFM image and (c) representative EDX analysis of PHMeDOT.

Figure 3. (a) Control voltammograms in 0.1 M PBS of bare GC, PHMeDOT as prepared, and PHMeDOT coated with GOx (PHMeDOT-GOx). (b) Current-time plot for PHMeDOT as prepared and PHMeDOT-GOx upon the successive addition of 1 mM glucose in 0.1 M PBS at polarization potential -600 mV vs Ag│AgCl.

Figure 4. Current-time plots for the PHMeDOT NEGS upon the successive addition in 0.1 M PBS of: (i) 1 mM UA, 1 mM AA, 1 mM DA and 1 mM glucose (blue profile); and (ii) 1 mM glucose (red profile). Polarization potential: -600 mV vs Ag│AgCl.

Figure 5. Current density response versus glucose concentration for PHMeDOT NEGSs. Error bars indicate standard deviations for eight measurements using independent electrodes. The calibration curve equation is also displayed.

Figure 6. Current-time plot registered after deposit two drops of blood onto the surface of a PHMeDOT non-enzymatic glucose sensor. Profiles correspond to the blood of two different individuals. The graphic of the inset indicates that the current density is perfectly equilibrated after 195 seconds. Polarization potential: -600 mV vs Ag│AgCl. The figure also displays the concentration of glucose measured using the OneTouch UltraMini® blood glucose meter, commercialized by the Johnson&Johnson company. The blood used to measure such concentrations correspond to the individuals 1 and 2 (marked with arrows). The concentration of glucose in blood is expressed in mg/dL.

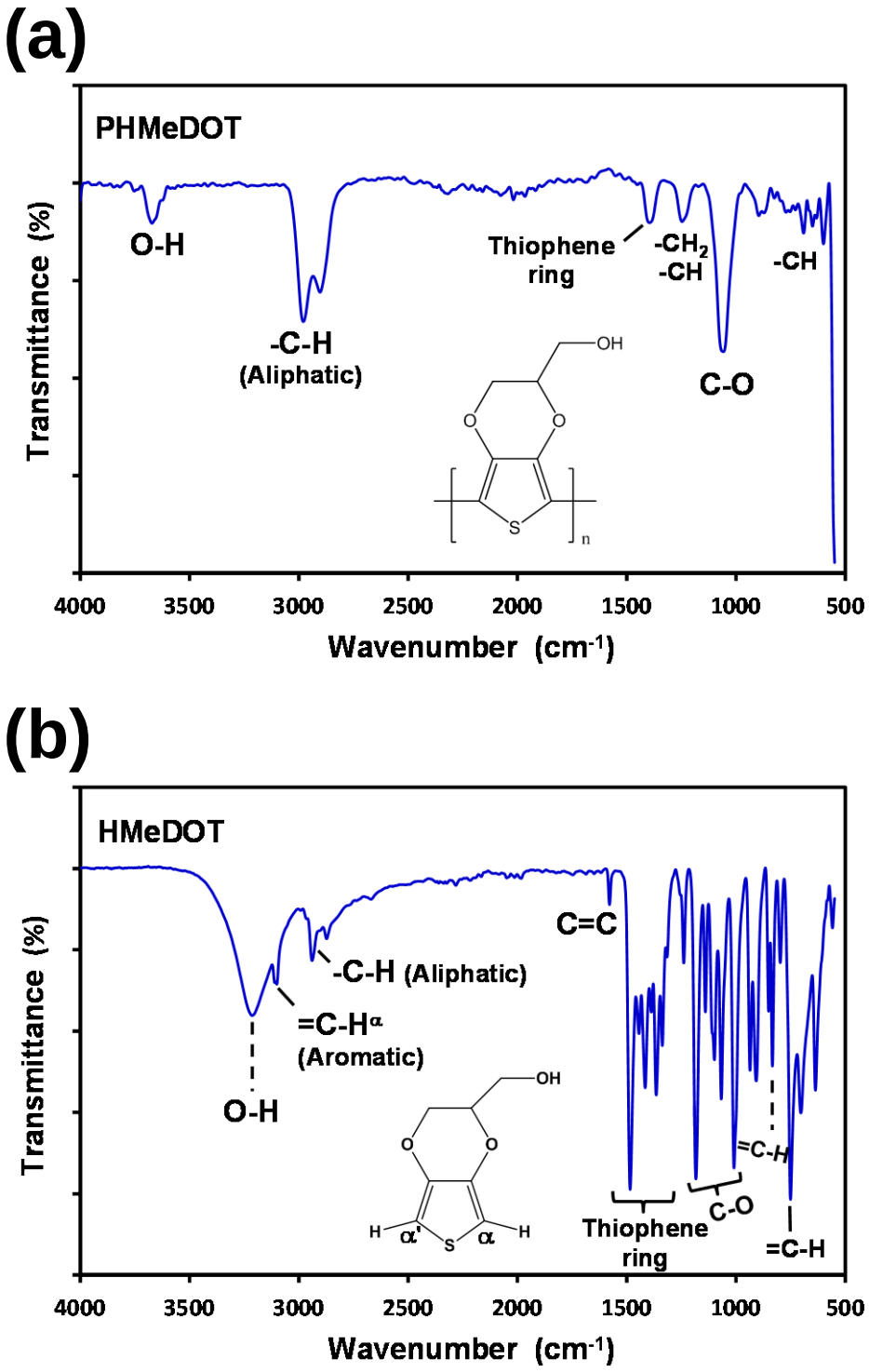
(a)
PHMeDOT
Transmittance (%)
O-H
-C-H
(Aliphatic)
Thiophene
ring
-CH2
-CH
-CH
C-O
OH
O
O
S
n
4000
3500
3000
2500
2000
1500
1000
500
Wavenumber (cm-1)
(b)
HMeDOT
Transmittance (%)
C=C
-C-H (Aliphatic)
=C-Hα
(Aromatic)
O-H
OH
O
O
H
α'
S
α
H
=C-H
C-O
Thiophene
ring
=C-H
4000
3500
3000
2500
2000
1500
1000
500
Wavenumber (cm-1)

Figure 1

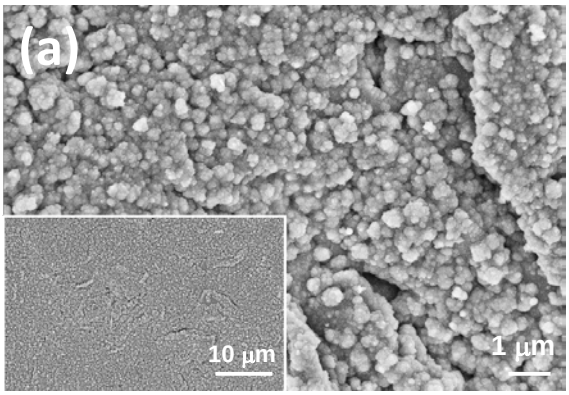

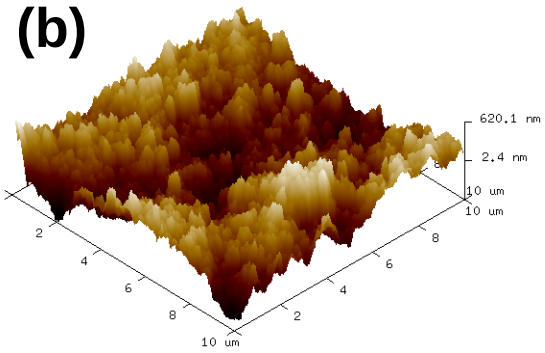

(c)

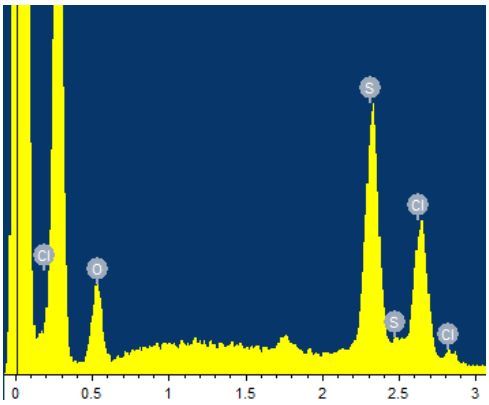

Element	Weight	Atomic
C	41.77	64.07
O	3.37	3.98
S	28.47	16.71
Cl	26.39	14.52

Figure 2

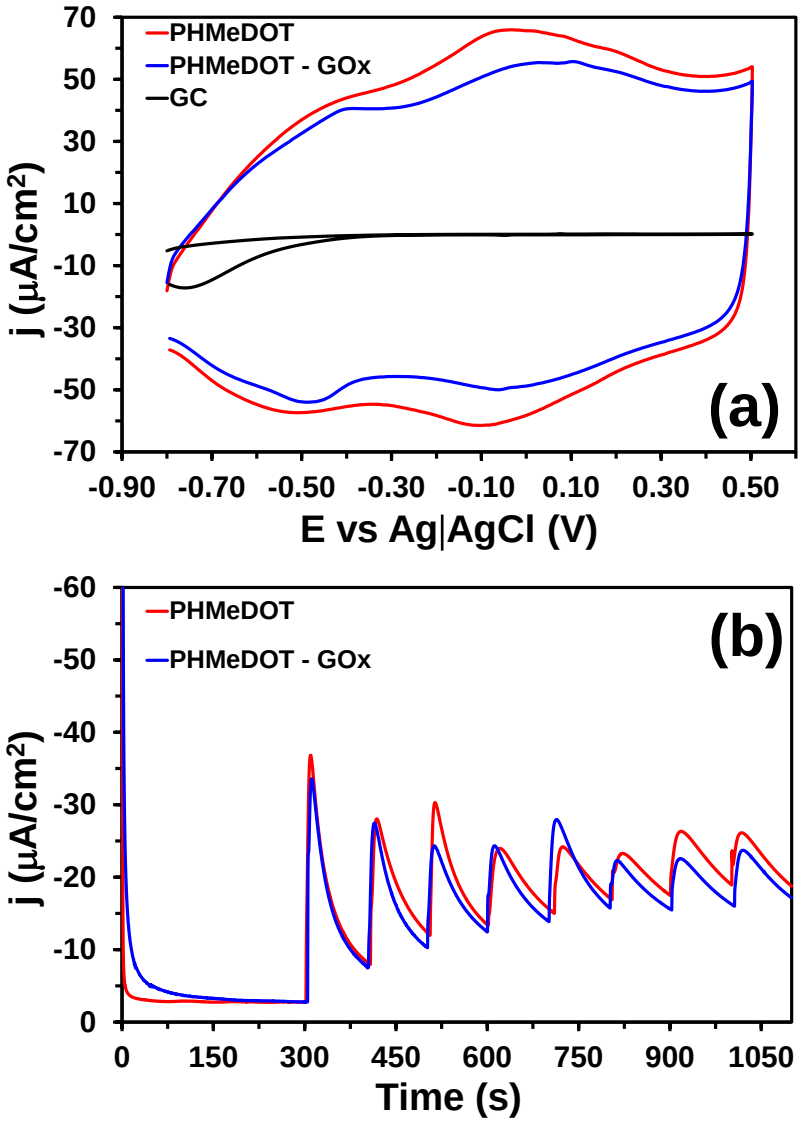
PHMeDOT
PHMeDOT - GOx
GC
(a)
j (µA/cm²)
E vs Ag|AgCl (V)
(b)
PHMeDOT
PHMeDOT - GOx
j (µA/cm²)
Time (s)

Figure 3

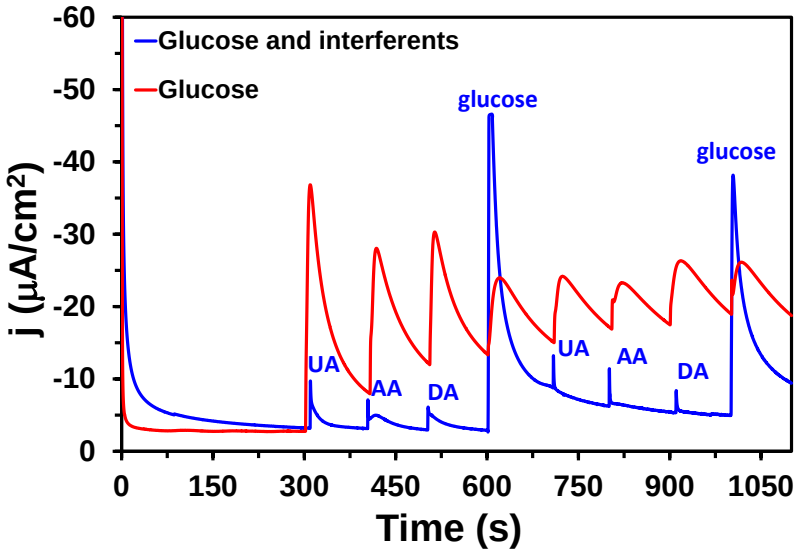
Glucose and interferents
Glucose
glucose
glucose
UA
AA
DA
UA
AA
DA
j (μA/cm²)
Time (s)
-60
-50
-40
-30
-20
-10
0
0
150
300
450
600
750
900
1050

Figure 4

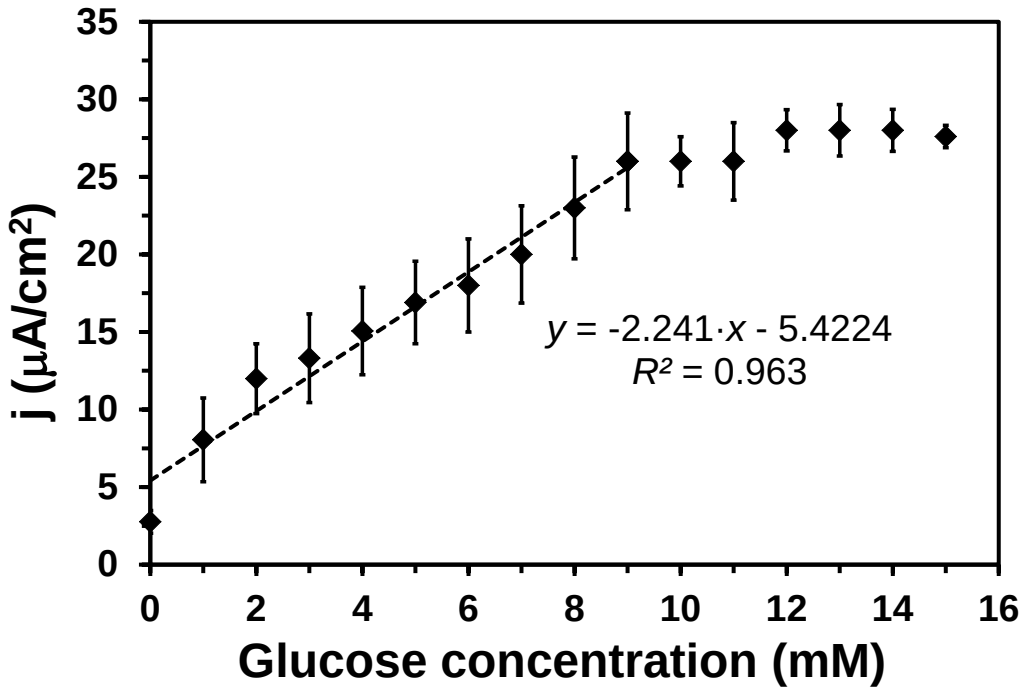
35
30
25
20
15
10
5
0
j (μA/cm²)
0
2
4
6
8
10
12
14
16
Glucose concentration (mM)
y = -2.241·x - 5.4224
R² = 0.963

Figure 5

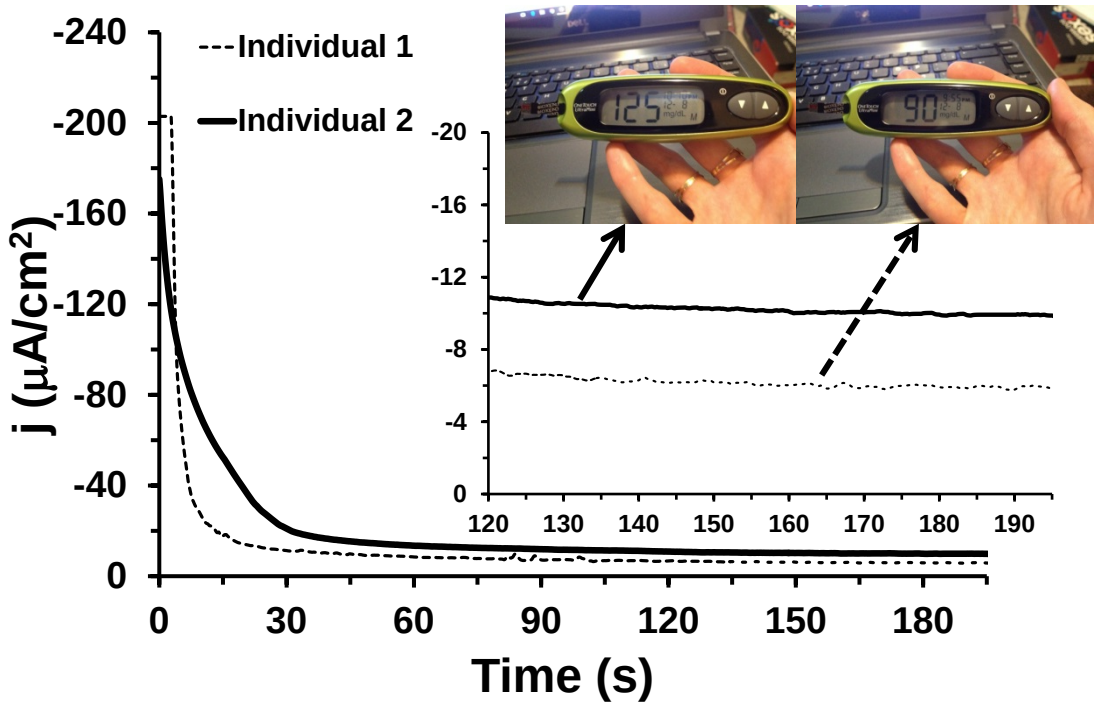
-240
-200
-160
-120
-80
-40
0
j (μA/cm²)
---Individual 1
Individual 2
0
30
60
90
120
150
180
Time (s)
-20
-16
-12
-8
-4
0
120
130
140
150
160
170
180
190
125
90

Figure 6

Graphical Abstract